GEORG-AUGUST-UNIVERSITÄT
GÖTTINGEN

Lectures on thermalization in closed quantum many-body systems

Stefan Kehrein
Institut für Theoretische Physik, Universität Göttingen

These slides are supplementary material
and **not** a self-contained presentation.

1. Thermalization in closed quantum many-body systems: Experiments

Ultracold gases

Isolation from environment

Bloch group
http://www.quantum-munich.de/media/nice-photos/

Lattice control

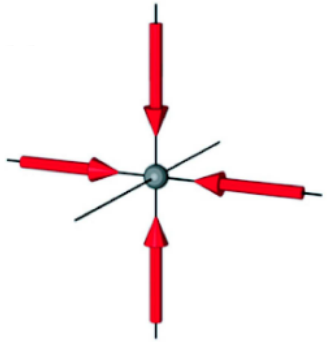

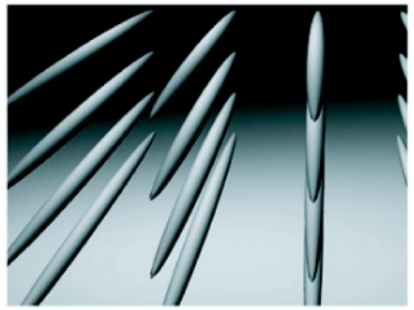

Interaction control

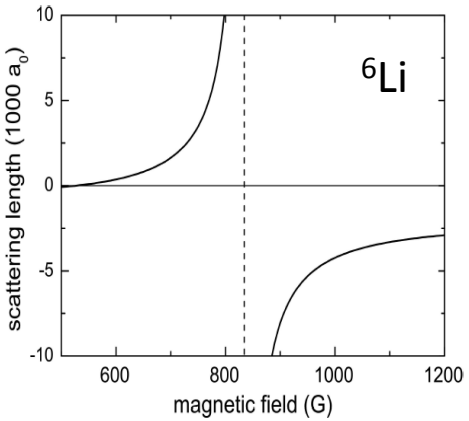

I. Bloch et al., Rev. Mod. Phys. 80 (2008)

Quantum Newton's Cradle

Kinoshita et al., Nature 440 (2006)

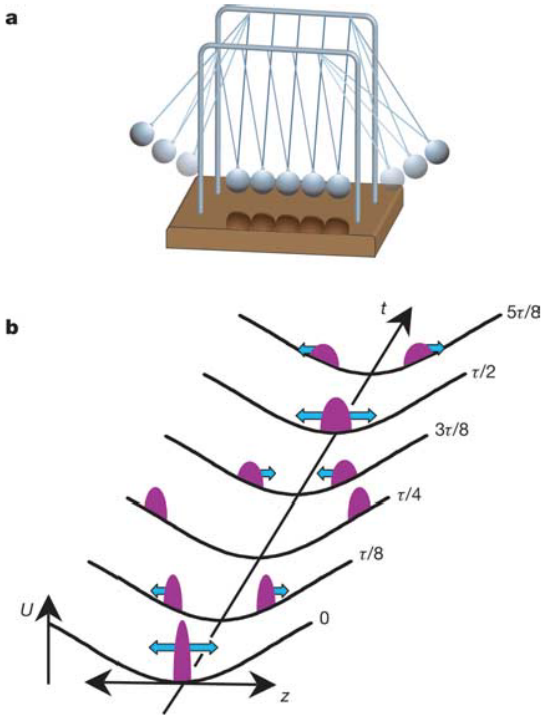

Figure 1 | Classical and quantum Newton's cradles. **a**, Diagram of a classical Newton's cradle. **b**, Sketches at various times of two out of equilibrium clouds of atoms in a 1D anharmonic trap, $U(z)$. At time $t = 0$, the atoms are put into a momentum superposition with $2\hbar k$ to the right and $2\hbar k$ to the left. The two parts of the wavefunction oscillate out of phase with each other with a period τ. Each atom collides with the opposite momentum group twice every full cycle, for instance, at $t = 0$ and $\tau/2$. Anharmonicity causes each group to gradually expand, until ultimately the atoms have fully dephased. Even after dephasing, each atom still collides with half the other atoms twice each cycle.

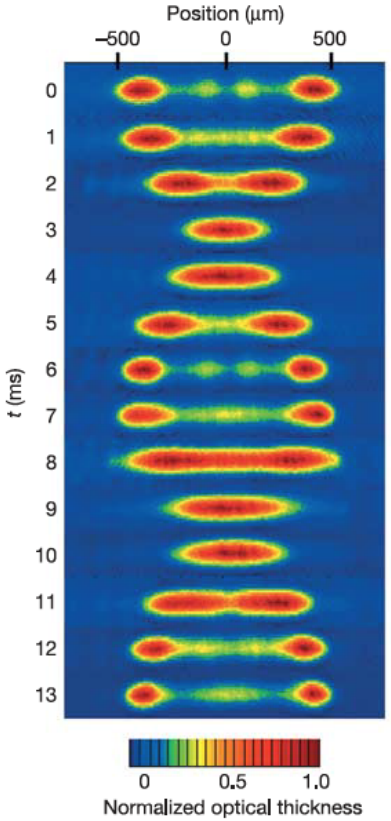

2 | Absorption images in the first oscillation cycle for initial average oupling strength $\gamma_o = 1$. Atoms are always confined to one

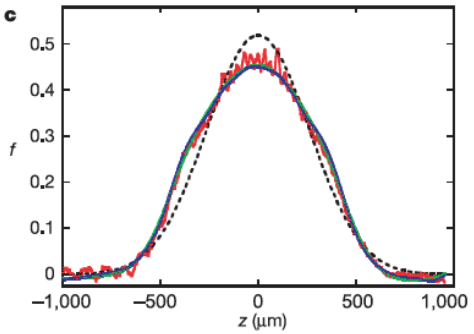

Figure 4 | Projected versus actual $f(p_{ex})$ for various γ_d, the dephased average peak coupling strength. The blue and green curves are $f(p_{ex})$ for $t_o = 15\tau$, rescaled to account for loss and convolved with the known heating during t_{obs}. The blue curve's heating model is more sophisticated than that of the green curve, but the results are insensitive to the details. The red curves are the actual distributions at $t_o + t_{obs}$. **a**, $\gamma_d = 18$ and $t_{obs} = 15\tau$. **b**, $\gamma_d = 3.2$ and $t_{obs} = 25\tau$. **c**, $\gamma_d = 1.4$ and $t_{obs} = 25\tau$. The dashed line in **c** is a gaussian with the same number of atoms and r.m.s. width as the actual distribution. To the extent that the actual distribution conforms to the projected distribution rather than to a gaussian, the atoms have not thermalized.

Lieb-Liniger model: $$H = -\sum_{j=1}^{N} \frac{\partial^2}{\partial x_j^2} + 2c \sum_{i<j} \delta(x_i - x_j)$$

Time-resolved PES

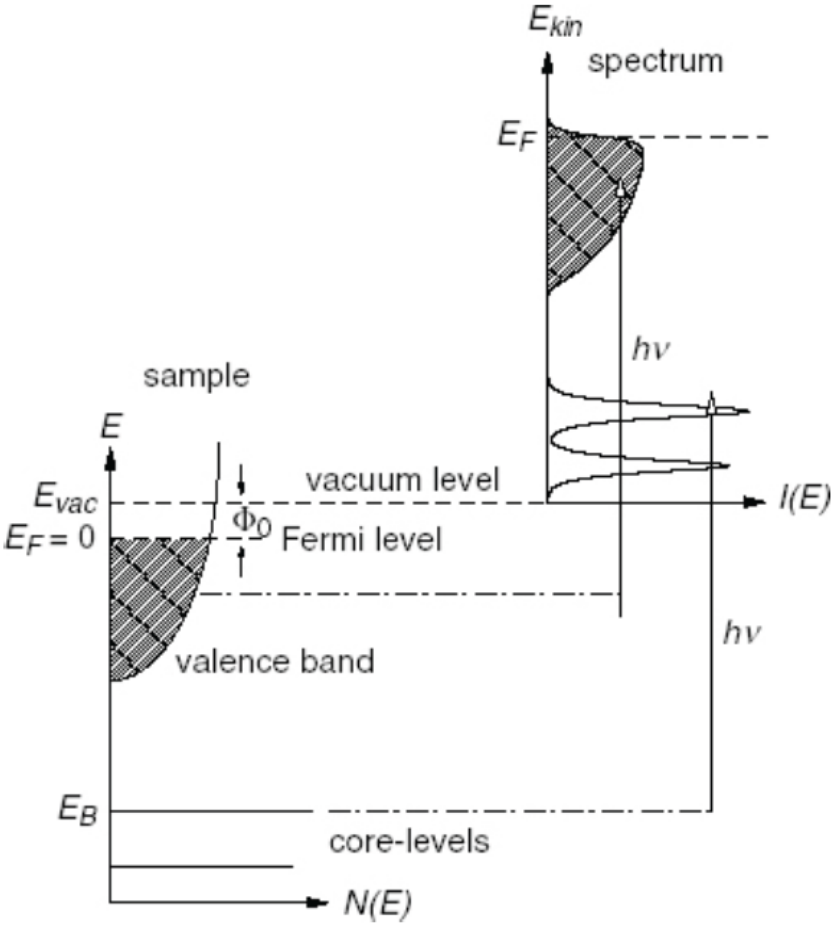

F. Reinert et al., New J. Phys. 7 (2005)

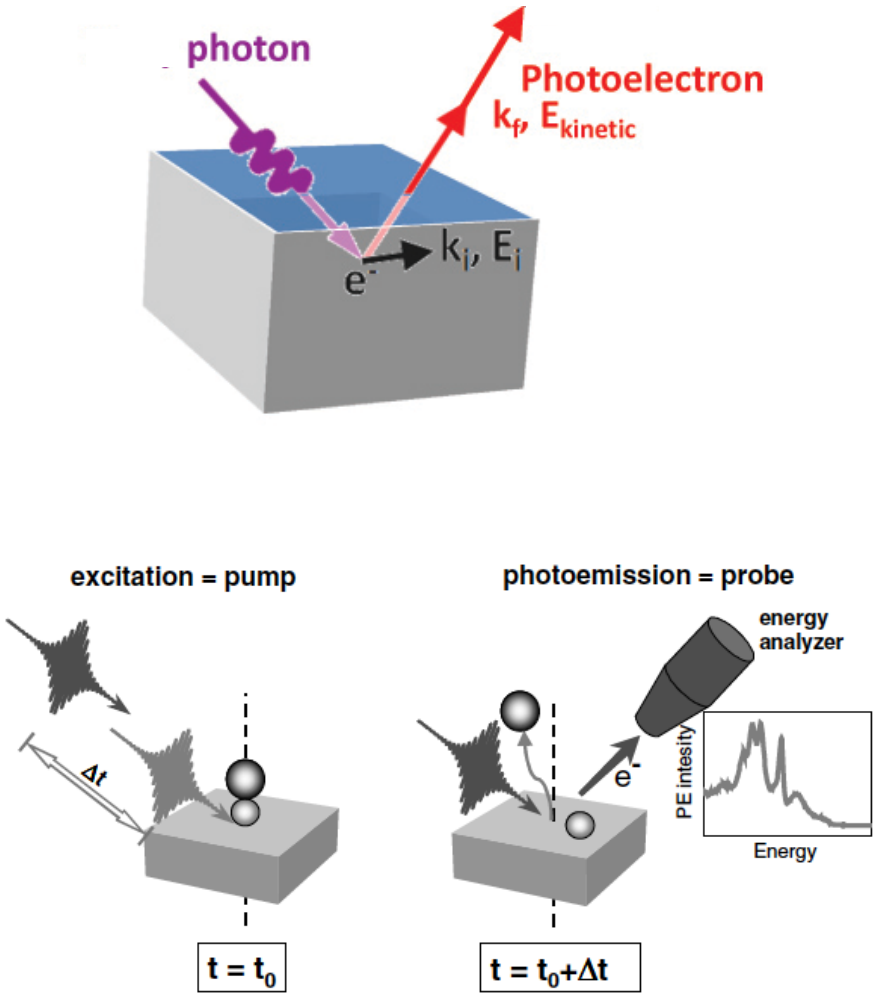

M. Bauer, J. Phys. D 38 (2005)

W. S. Fann et al.,
Phys. Rev. B46 (1992)

Time-resolved PES on gold
at room temperature

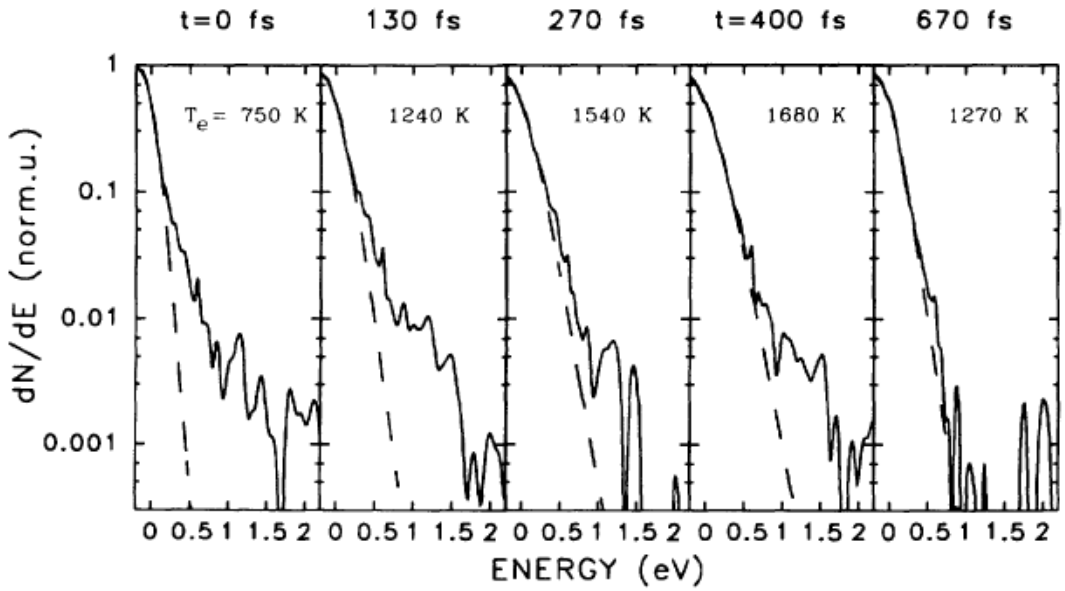

FIG. 2. Electron energy distribution function vs energy with 300 μJ/cm^2 absorbed laser fluence at five time delays.

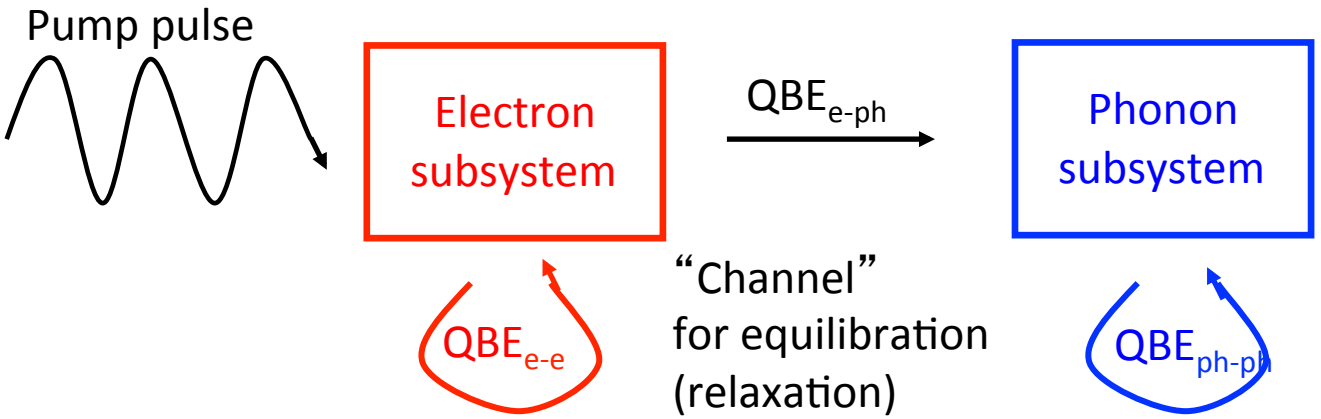

2. The Fermi-Pasta-Ulam-Tsingou problem

E. Fermi, J. Pasta, S. Ulam;
Los Alamos Report (1955)

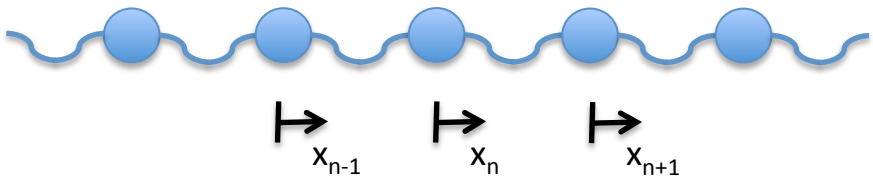

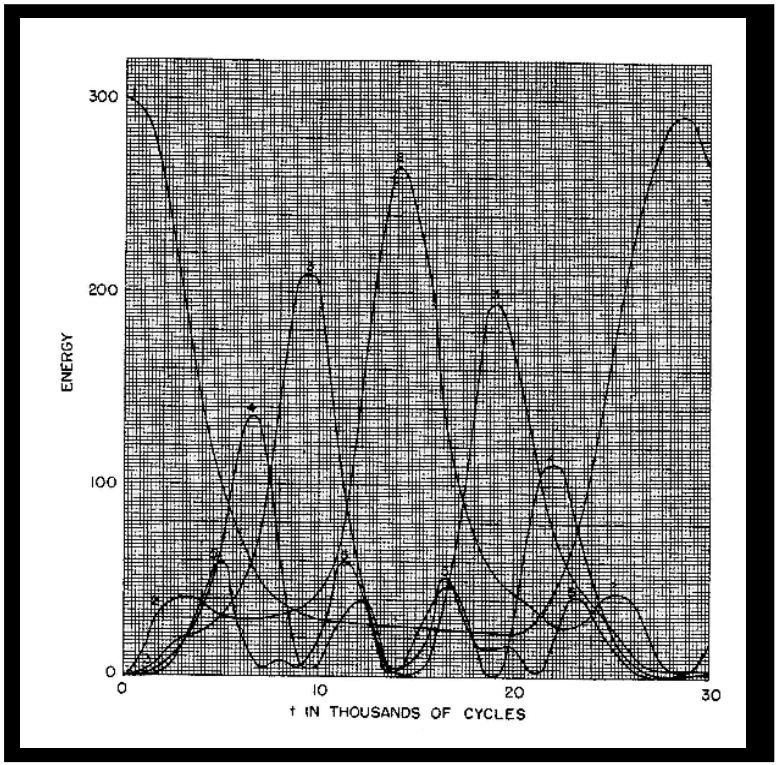

Initial state: Mode k=1 excited

$$\frac{d^2x_n}{dt^2} = (x_{n+1} - 2x_n + x_{n-1}) + \alpha \left[(x_{n+1} - x_n)^2 - (x_n - x_{n-1})^2\right] + \beta \left[(x_{n+1} - x_n)^3 - (x_n - x_{n-1})^3\right]$$

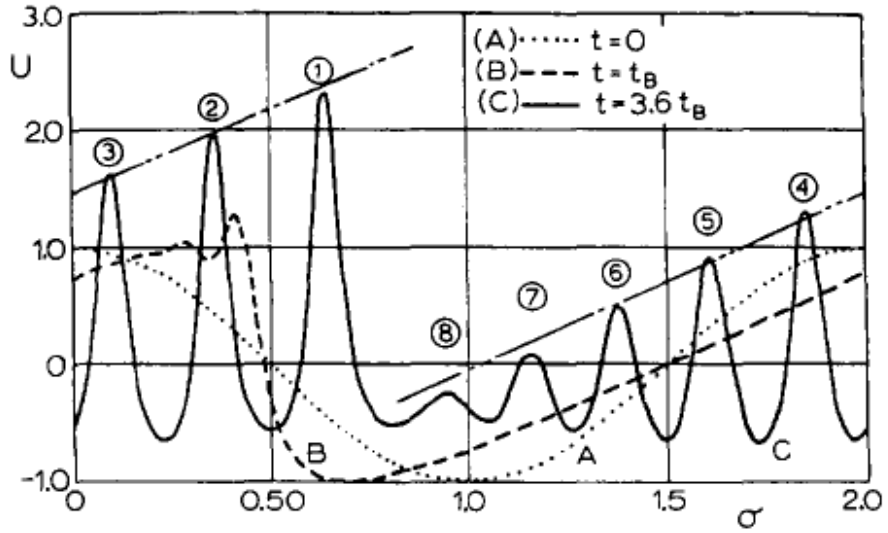

Fig. 8. The numerically integrated solution of the KdV equation for an initial condition taken as one period of a cosine, which here appears as the dotted curve. The shape of the time-evolved curve at a later time is shown as the dashed curve. Finally, the solid curve reveals that the initial cosine excitation has broken up into eight solitons which move with speeds proportional to their heights. The various FPU recurrences now find their explanation in terms of the recurrences which occur as these eight solitons move with incommensurate speeds around a circle.

3. Integrable vs. non-integrable quantum systems

D. A. Rabson et al., Phys. Rev. B 69 (2004)

Integrable Hamiltonian

$$H_{XXZ}=\frac{1}{2}\sum_{i=1}^{N}\left(e^{i\varphi/N}S_i^+S_{i+1}^-+e^{-i\varphi/N}S_i^-S_{i+1}^+\right)$$

$$+\sum_{i=1}^{N}J_1S_i^zS_{i+1}^z\,.$$

Non-integrable perturbation

$$\delta H=\sum_{i=1}^{N}J_2S_i^zS_{i+2}^z$$

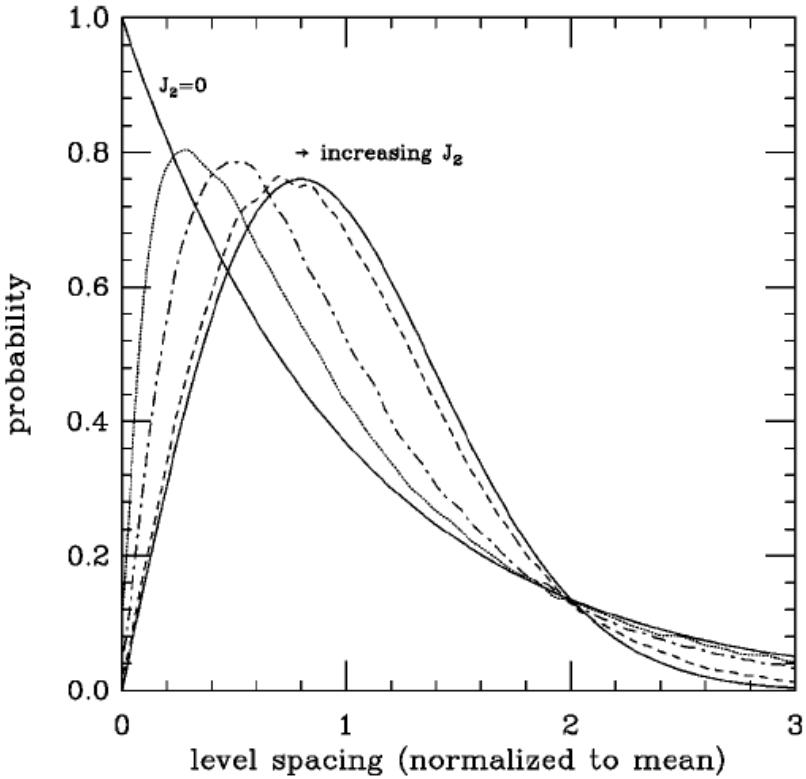

FIG. 1. Typical crossover of the level-spacing distribution from Poisson (left solid curve) for $J_2=0$ to Wigner-Dyson (right solid curve) for a representative system. The plot is made for $N=18$, $S^z=3$, $J_1=0.2$, momentum $k=0$, and $J_2=0.1,0.2,0.5$. For $J_2=0$ the numerical distribution agrees very closely with the exponential plotted. The Wigner-Dyson distribution shown is the theoretical curve for the orthogonal ensemble.

5. Thermalization in integrable systems: GGE

M. Fagotti and F. Essler; Phys. Rev. B 87 (2014), arXiv:1302.6944

Transverse field Ising model: $$H(h) = -\sum_{i=1}^{N-1} \sigma_i^z \, \sigma_{i+1}^z + h \sum_{i=1}^{N} \sigma_i^x$$

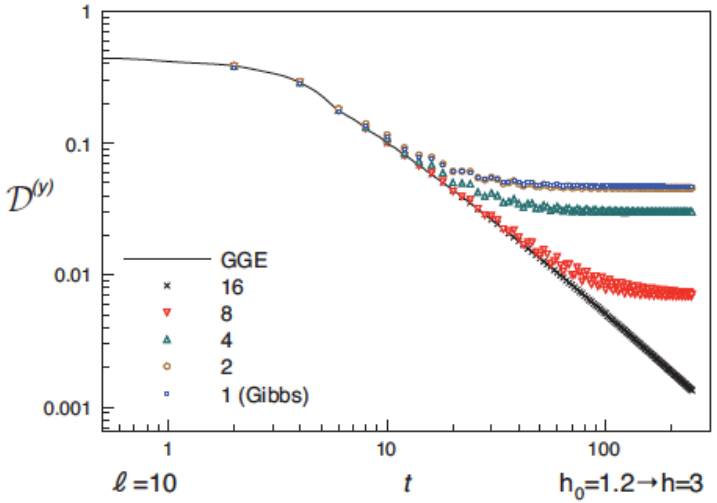

FIG. 6: Distance $\mathcal{D}^{(y)} = \mathcal{D}(\rho_\ell(t), \rho^{(y)}_{\mathrm{tGGE},\ell})$ at fixed length $\ell = 10$ between quench and truncated GGE reduced density matrices for $y = 1, 2, 4, 8, 16$ and a quench within the paramagnetic phase. Here y is the maximal range of the densities of local conservation laws included in the definition of the ensemble. As the number of conservation laws is increased, the time window, in which the distance decays as $t^{-3/2}$, increases. At very late times all distances with finite y saturate to nonzero values.

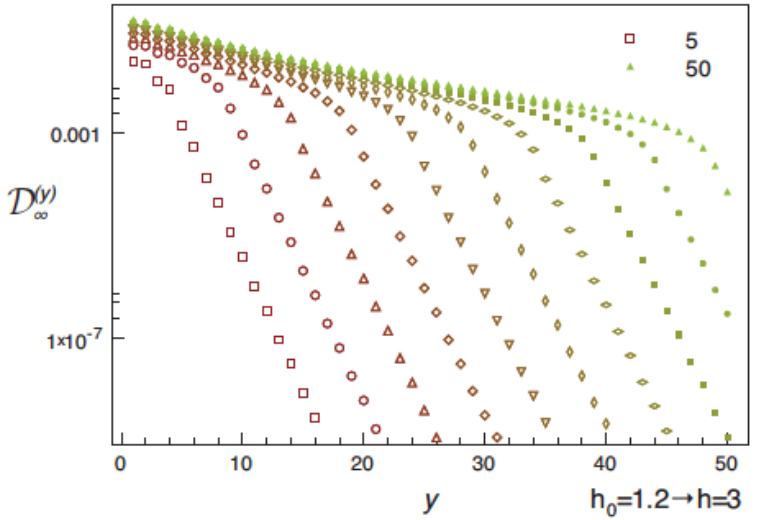

FIG. 7: Distance $\mathcal{D}^{(y)}_\infty = \mathcal{D}(\rho_{GGE,\ell}, \rho^{(y)}_{tGGE,\ell})$ between the GGE and the truncated GGEs obtained by imposing local conservation laws with densities involving at most $y+1$ consecutive sites. The quench is from $h_0 = 1.2$ to $h = 3$ and the subsystem size ranges from $\ell = 5$ to $\ell = 50$. Colors and sizes change gradually as a function of the size ℓ. For $y > \ell$, the distance starts decaying exponentially in y, with an ℓ-independent decay constant.

Transverse field Ising model:

$$H(h) = -\sum_{i=1}^{N-1} \sigma_i^z \, \sigma_{i+1}^z + h \sum_{i=1}^{N} \sigma_i^x$$

Ising interaction — transverse magnetic field

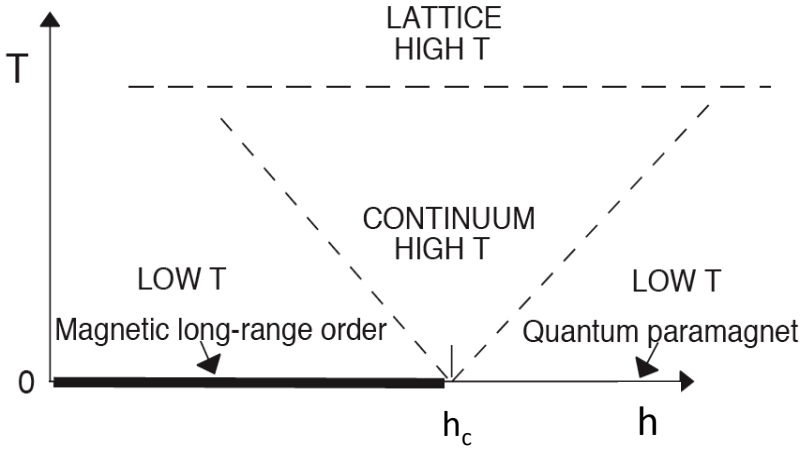

- Quantum phase transition at $h_c = 1$
- Integrable model:
  Quadratic in fermions after Jordan-Wigner transformation

S. Sachdev, Quantum Phase Transitions (Cambridge Univ. Press, 2011)

7. ETH: Evidence and implications

M. Rigol et al., Nature 452 (2008)

Hard core bosons on 2d lattice

Hard core bosons in 1d with pbc

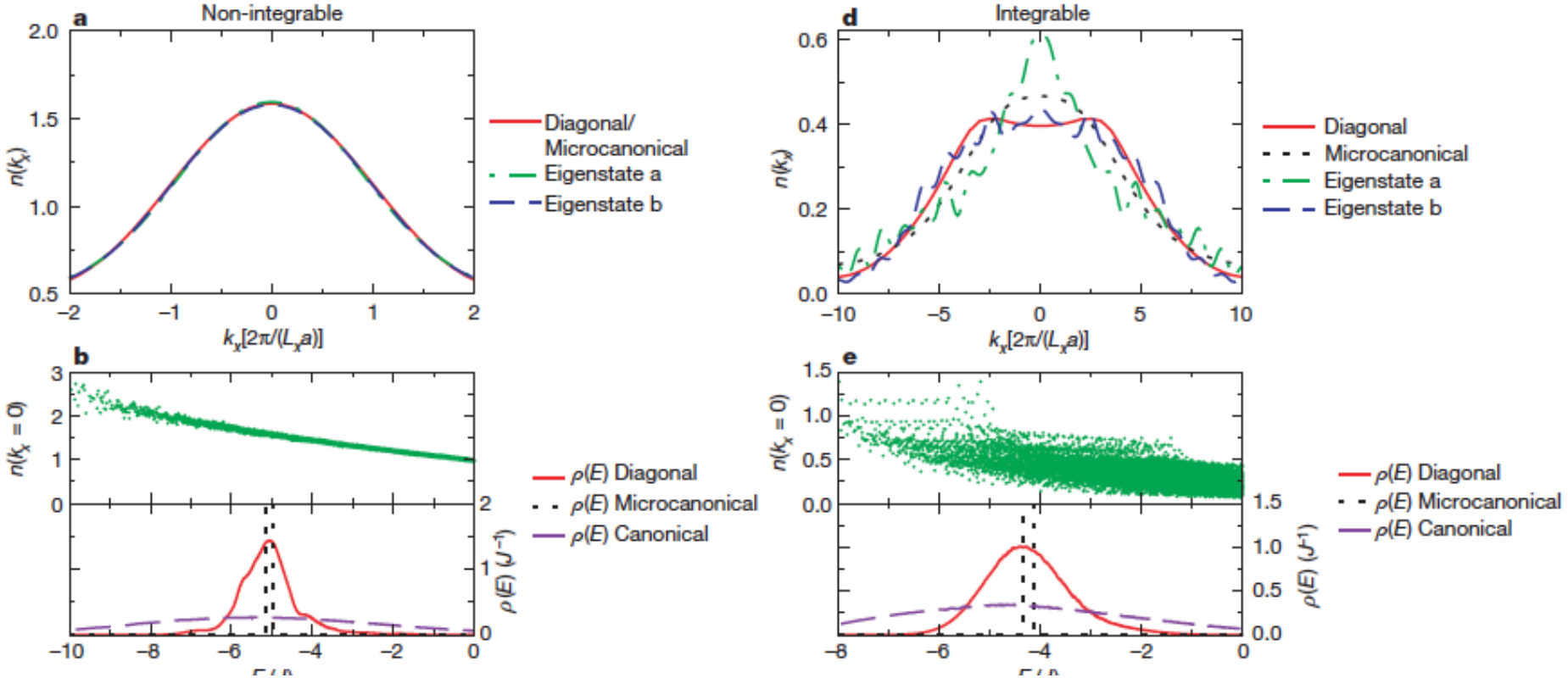

Figure 3 | Eigenstate thermalization hypothesis. **a**, In our non-integrable system, the momentum distribution $n(k_x)$ for two typical eigenstates with energies close to E_0 is identical to the microcanonical result, in accordance with the ETH. **b**, Upper panel: the EEV $n(k_x = 0)$, considered as a function of the eigenstate energy resembles a smooth curve. Lower panel: the energy distributions $\rho(E)$ (in units of J^{-1}) of the three ensembles we consider here. **c**, Detailed view of $n(k_x = 0)$ (left-hand scale) and $|C_\alpha|^2$ (right-hand scale) for 20 eigenstates around E_0. **d**, In the integrable system, the values of $n(k_x)$ for two eigenstates, a and b, with energies close to E_0 and for the microcanonical and diagonal ensembles are very different from each other; that is, the ETH fails. **e**, Upper panel: the EEV $n(k_x = 0)$, considered as a function of the eigenstate energy gives a thick cloud of points rather than resembling a smooth curve. Lower panel: the energy distributions in the integrable system are similar to the non-integrable ones depicted in **b**. **f**, Correlation between $n(k_x = 0)$ and $|C_\alpha|^2$ for 20 eigenstates around E_0. This correlation explains why in **d** the microcanonical prediction for $n(k_x = 0)$ is larger than the diagonal one.

L. D'Alessio et al.; Adv. Phys. 65 (2016); arXiv:1509.06411

Hard core bosons in 1d with pbc:

$$\hat{H} = \sum_{j=1}^{L} \Big[-J \left(\hat{b}_j^\dagger \hat{b}_{j+1} + \text{H.c.} \right) + V \left(\hat{n}_j - \frac{1}{2} \right) \left(\hat{n}_{j+1} - \frac{1}{2} \right) - J' \left(\hat{b}_j^\dagger \hat{b}_{j+2} + \text{H.c.} \right) + V' \left(\hat{n}_j - \frac{1}{2} \right) \left(\hat{n}_{j+2} - \frac{1}{2} \right) \Big]$$

Integrable

non-integrable

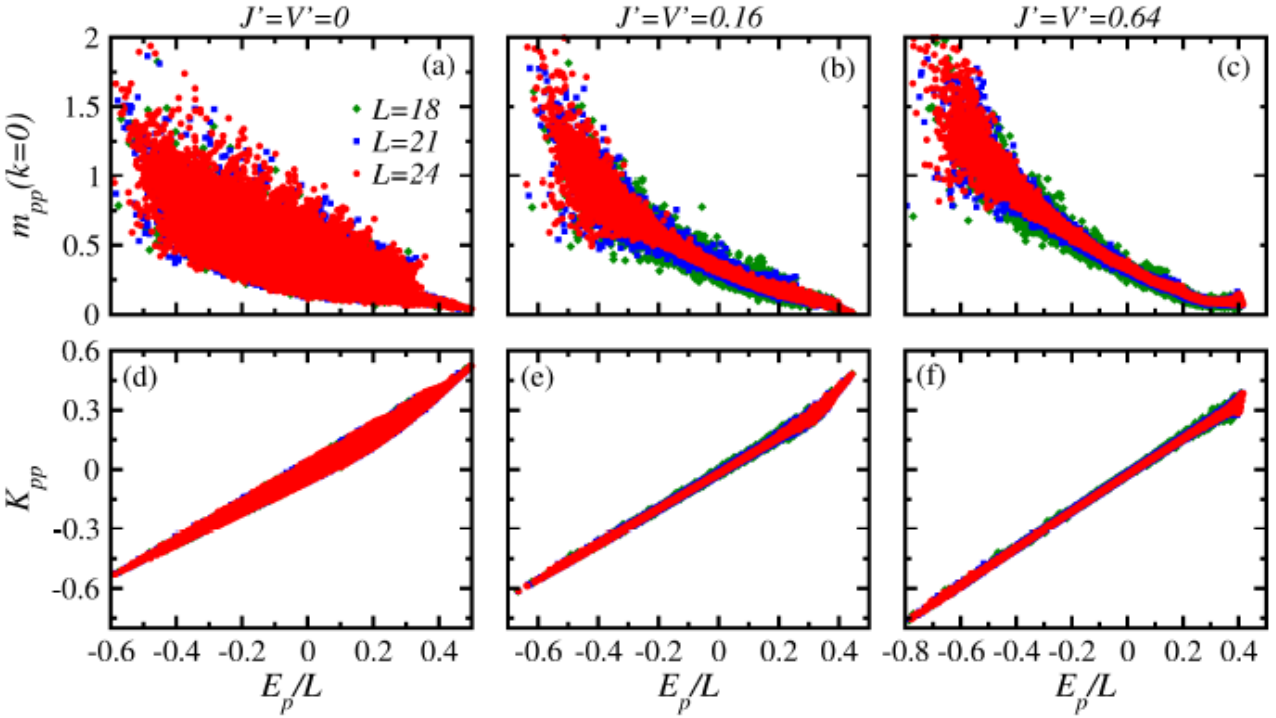

Zero momentum mode occupation

Kinetic energy/site

Figure 13. Eigenstate expectation values of the occupation of the zero momentum mode [(a)–(c)] and the kinetic energy per site [(d)–(f)] of hard-core bosons as a function of the energy per site of each eigenstate in the entire spectrum, that is, the results for all k-sectors are included. We report results for three system sizes ($L = 18$, 21, and 24), a total number of particles $N = L/3$, and for two values of $J' = V'$ [$J' = V' = 0.16$ in panels (b) and (e) and $J' = V' = 0.64$ in panels (c) and (f)] as one departs from the integrable point [$J' = V' = 0$ in panels (a) and (d)]. In all cases $J = V = 1$ (unit of energy). See also Ref. [157].

M. Rigol et al., Nature 452 (2008)

Classical thermalization: Thermal state does not resemble initial state

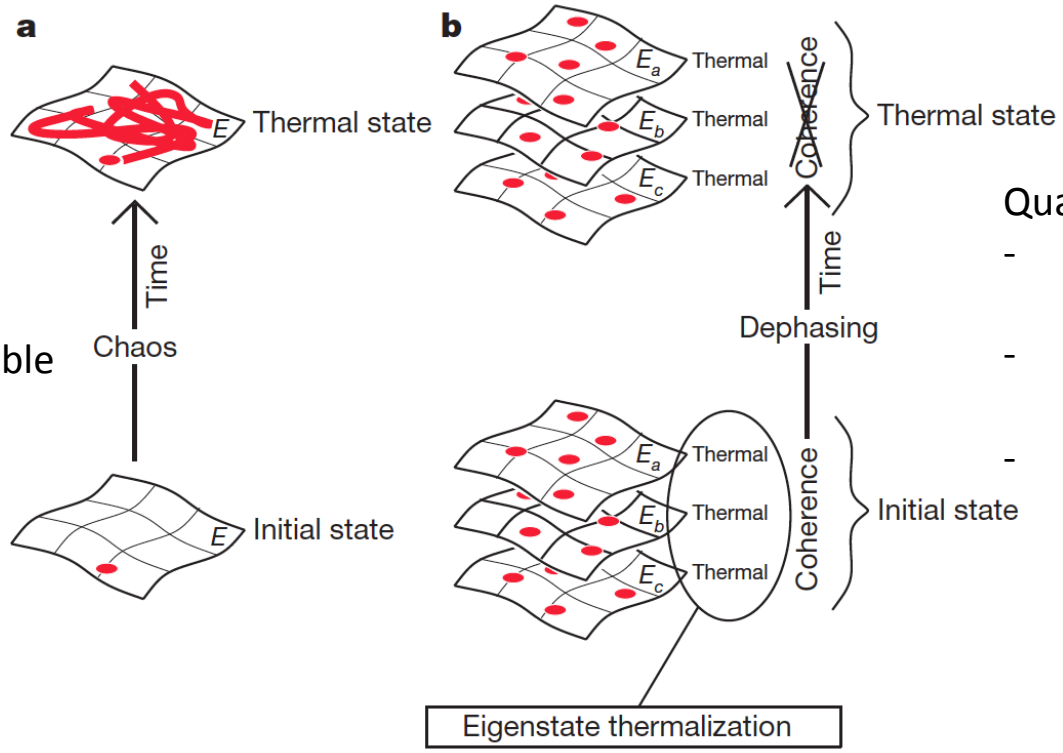

Quantum thermalization (ETH):

- Every eigenstate of the Hamiltonian is thermal
- Thermal nature initially hidden due to coherences
- Dephasing leads to effectively incoherent superposition of thermal states, weights of these states unimportant

8. Prethermalization

M. Moeckel and S. Kehrein, Phys. Rev. Lett. 100 (2008); Ann. Phys. 324 (2009); New. J. Phys. 12 (2010)

Landau Fermi liquid theory:

Adiabatic switching on of interaction (closed system)
→ 1 to 1 correspondence between physical electrons and quasiparticles

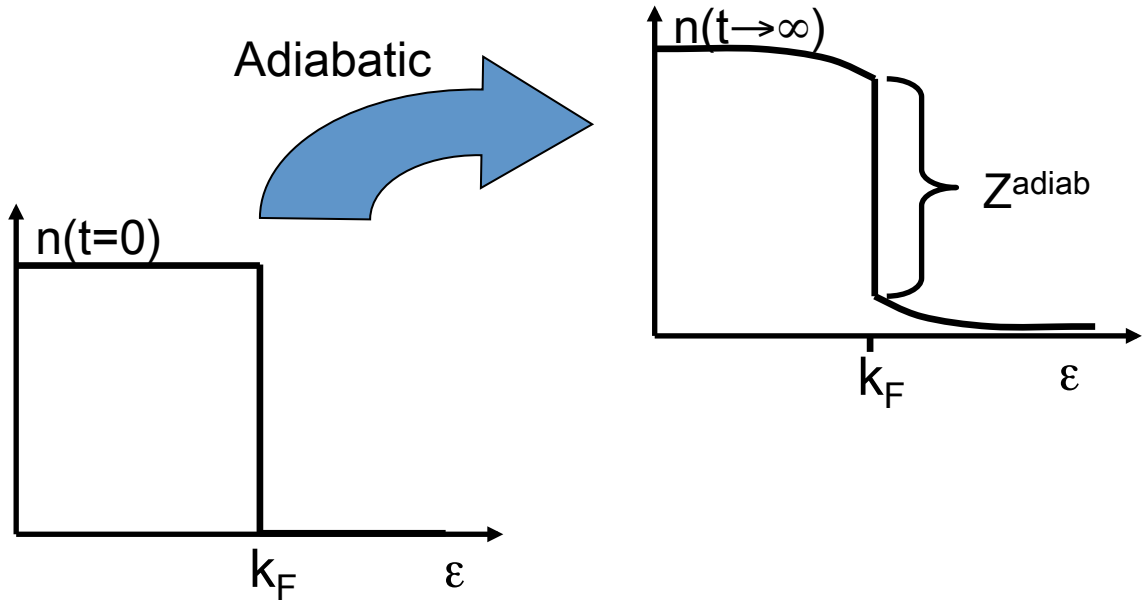

What happens for sudden switching/ away from the adiabatic limit?

Novel metastable state (prethermalized state) with non-equilibrium quasiparticle residue

$$Z^{inst} \neq Z^{adiab}$$

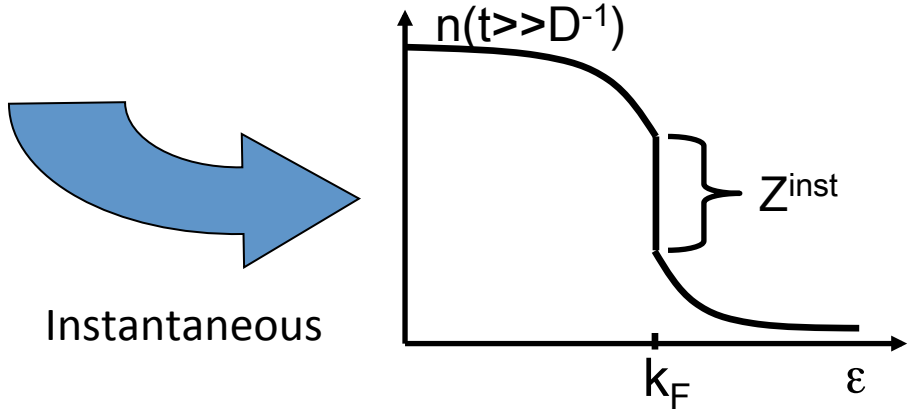

- Prethermalized state with $1-Z^{inst} = 2\,(1-Z^{adiab})$
  [similar prethermalized states have been found in many other models]

- On longer timescale prethermalized state develops to thermal state
  (thermal Fermi-Dirac distribution of electrons)

- Temperature depends on non-adiabacity

Numerical confirmation: Non-equilibrium DMFT with real time Quantum Monte Carlo
M. Eckstein et al., Phys. Rev. Lett. 103 (2009)

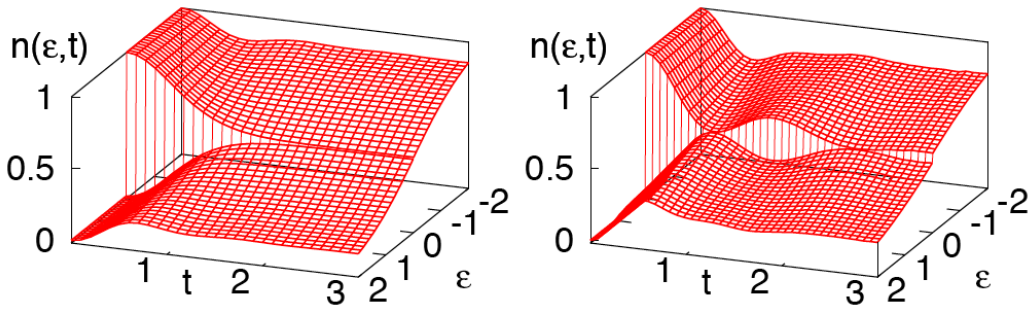

FIG. 1: Momentum distribution $n(\epsilon_{\boldsymbol{k}}, t)$ for quenches from $U = 0$ to $U = 3$ (left panel) and $U = 5$ (right panel).

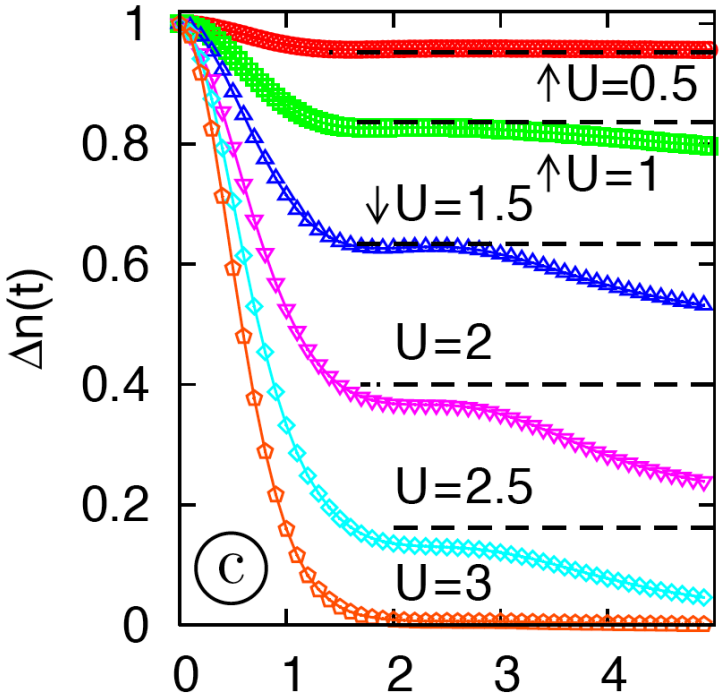

9. Outlook & Key Questions

- ETH: Better (analytical) understanding
- Reversibility vs. irreversibility
- Periodically/quasiperiodically driven systems:
  Steady states, prethermalization
- Method development for real time evolution: esp. d>1
- Hydrodynamic long-time tails: Global equilibration

Hydrodynamic long-time tails: J. Lux et al., arXiv:1311.7644

1d bosonic Hubbard model: Weak quench in regime U>>J

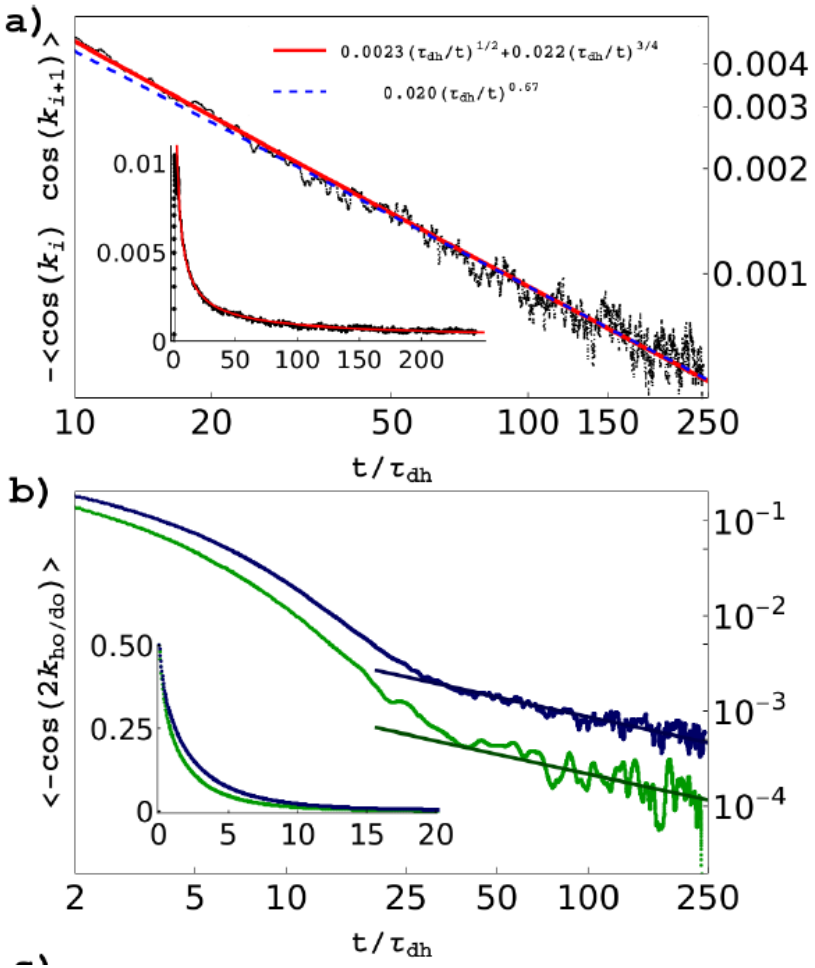

John von Neumann once referred to the theory of non-equilibrium systems as the *theory of non-elephants*.

Nevertheless, we shall attempt such a theory of non-elephants.

(P. Bak and M. Paczuski, Proc. Natl. Acad. Sci. USA 92, 1995)